European Journal of Medicinal Chemistry 60 (2013) 29–41

Contents lists available at SciVerse ScienceDirect

European Journal of Medicinal Chemistry

journal homepage: http://www.elsevier.com/locate/ejmech

Original article

Structure-based design, synthesis and evaluation of novel anthra[1,2-*d*]imidazole-6,11-dione derivatives as telomerase inhibitors and potential for cancer polypharmacology

Chun-Liang Chen [a], Deh-Ming Chang [a,c], Tsung-Chih Chen [a], Chia-Chung Lee [a], Hsi-Hsien Hsieh [e], Fong-Chun Huang [e], Kuo-Feng Huang [f], Jih-Hwa Guh [g], Jing-Jer Lin [e,h,**], Hsu-Shan Huang [a,b,d,*]

[a] *Graduate Institute of Life Sciences, National Defense Medical Center, Taipei 114, Taiwan*
[b] *School of Pharmacy, National Defense Medical Center, Taipei 114, Taiwan*
[c] *Rheumatology/Immunology/Allergy, Tri-Service General Hospital, National Defense Medical Center, Taipei 114, Taiwan*
[d] *Department of Pharmacy Practice, Tri-Service General Hospital, National Defense Medical Center, Taipei 114, Taiwan*
[e] *Institute of Biopharmaceutical Sciences, National Yang-Ming University, Taipei 112, Taiwan*
[f] *Chi-Mei Medical Center, Tainan 710, Taiwan*
[g] *School of Pharmacy, National Taiwan University College of Medicine, Taipei 100, Taiwan*
[h] *Institute of Biochemistry and Molecular Biology, National Taiwan University College of Medicine, Taipei 100, Taiwan*

ARTICLE INFO

Article history:
Received 24 August 2012
Received in revised form
12 November 2012
Accepted 22 November 2012
Available online 29 November 2012

Keywords:
Telomerase
Imidazole-fused anthraquinones
TRAP assay
SEAP assay
Polypharmacology

ABSTRACT

A series of anthra[1,2-*d*]imidazole-6,11-dione derivatives were synthesized and evaluated for telomerase inhibition, *hTERT* expression and suppression of cancer cell growth *in vitro*. All of the compounds tested, except for compounds **4**, **7**, **16**, **24**, **27** and **28** were selected by the NCI screening system. Among them, compounds **16**, **39**, and **40** repressed *hTERT* expression without greatly affecting cell growth, suggesting for the selectivity toward *hTERT* expression. Taken together, our findings indicated that the analysis of cytotoxicity and telomerase inhibition might provide information applicable for further developing potential telomerase and polypharmacological targeting strategy.

1. Introduction

The anthracycline antibiotics daunorubicin, doxorubicin, mitoxantrone and ametantrone have been shown to process strong antiproliferative properties and clinically used to treat various cancers for many decades (Scheme 1) [1]. Recent studies illustrated anthracycline antibiotics might interrupt telomere maintenance through interfering the targeting of telomerase onto telomeres [2]. Telomeres are guanine-rich DNA sequences coated by specialized proteins at the terminal ends of eukaryotic chromosomes [3,4] which consists of hexameric TTAGGG repeats sequences in human cells [5]. Telomerase is a ribonucleoprotein that consists of a catalytic subunit (human telomerase reverse transcriptase, *hTERT*) and a template RNA (human telomerase RNA component, hTERC) to add telomere repeats to the 3′ single-strand overhang [6]. Extension of telomeres by telomerase is required for un-limited proliferation of most of the immortal and cancer cells [7,8]. The important roles of telomerase in cellular immortalization have made telomerase as a potentially molecular target for cancer therapeutic discovery which might have minimal side effects [9,10]. Moreover, the anthracycline antibiotics inhibit telomerase activities through the stabilizing of G-quadruplex structure sequences. It is also well accepted that human cancer cells achieve immortalization in large part through the illegitimate activation of telomerase expression [11,12]. Therefore, agents that suppress *hTERT* expression might further develop potential telomerase and polypharmacological targeting strategy.

Based on our previous studies, some of the 1,2-heteroannelated substitution on the anthraquinone and anthra[1,2-*d*]imidazole-

* Corresponding author. Department of Pharmacy Practice, Tri-Service General Hospital, National Defense Medical Center, Taipei 114, Taiwan. Tel.: +886 2 87923311x17327; fax: +886 2 87923169.
** Corresponding author. Institute of Biopharmaceutical Sciences, National Yang-Ming University, Taipei 112, Taiwan. Tel.: +886 2 28267000x5603; fax: +886 2 28267258.
E-mail addresses: jjlin@ym.edu.tw (J.-J. Lin), huanghs@ndmctsgh.edu.tw (H.-S. Huang).

0223-5234/$ – see front matter
http://dx.doi.org/10.1016/j.ejmech.2012.11.032

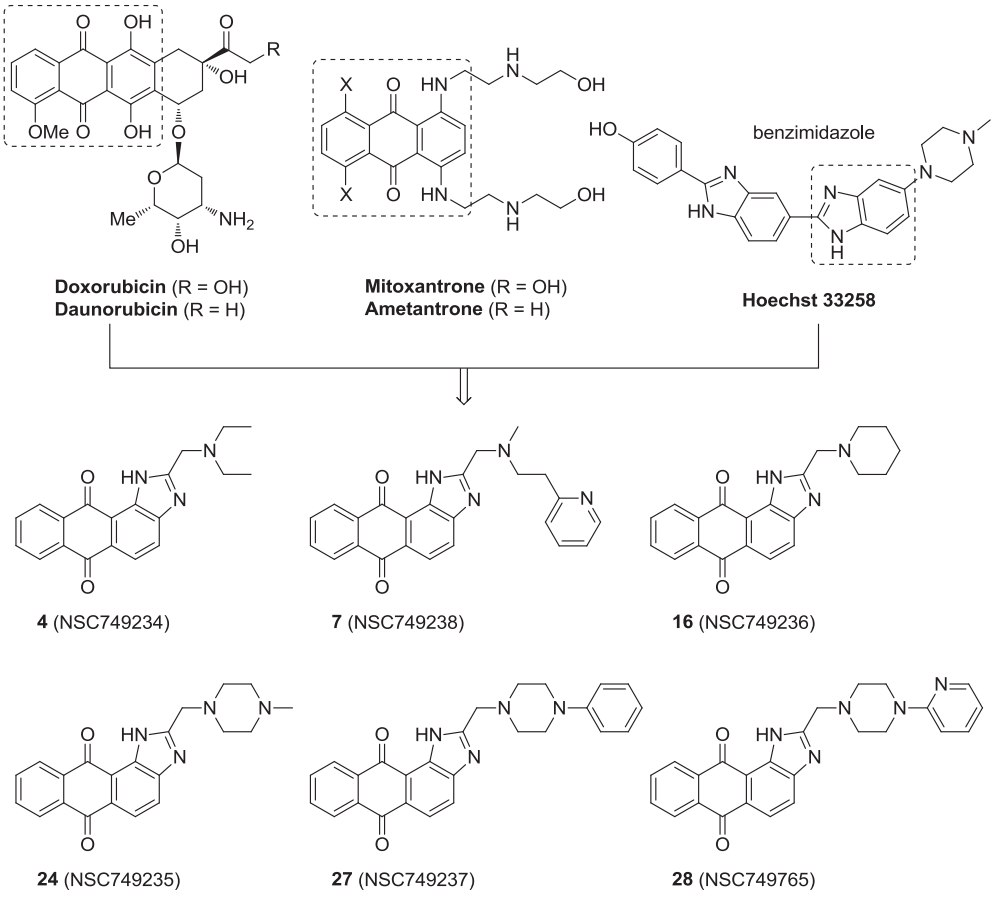

Scheme 1. Design of new compounds through hybridization of bioactive chromophoric anthraquinones (anthracycline antibiotic anticancer agents) and benzimidazole.

6,11-dione scaffold homologs might be interesting for cytotoxicity toward cancer cells or cancer polypharmacology [13]. Previous SARs studies have also shown that both anthraquinone-based compounds and bis-benzimidazole derivatives (Hoechst 33258) are known telomerase inhibitors or G-quadruplex stabilizers [14–16]. In the past, we also reported several results concerning the discovery of new classes of anthraquinone-linked heterocyclic derivatives [13,17–22]. Herein, we continue our efforts to develop an efficient synthetic procedure for the preparation of a novel series of *N*-substituent derivatives in the vacant 2-position of imidazole ring of anthra[1,2-*d*]imidazole-6,11-diones. In the series of designed analogs, we maintained benzimidazole as the central structure moiety since it was considered as the primary pharmacophore for potential telomerase inhibitory activity. Lead optimization were then focused on varying of other substituent moiety at the 2-position of the imidazole skeleton, by adding electron-withdrawing or electron-releasing substituents. These compounds were evaluated for cytotoxicity by MTT assay or sulforhodamine B assay (SRB assay) on non-small lung cancer cell, H1299, prostate cancer cells PC-3 [23–26], as well as telomerase inhibition using TRAP assay [27,28] and SEAP assay [29,30]. Finally, the interplay between the cytotoxicity, *hTERT* repressing activities and the drug explains the SARs of derivatives and the molecular basis of drug-induced activities.

2. Chemistry

There has been continuing interest in the synthesis of anthra[1,2-*d*]imidazole-6,11-dione derivatives and their systematic dissection largely on account of their biological activities [13]. The method for constructing the core structure of the compounds is outlined in Scheme 2. The synthesis commences starting from 1,2-diaminoanthraquinone, the cyclization with chloroacetyl chloride formed compound **1**. The preparation of compounds **2**–**33** involved direct amination using various amines and TEA/DIPEA in THF to obtain our desired derivatives. As shown in Scheme 2, compound **34** was prepared by amination between 1,2-diaminoanthraquinone and 3-chloropropionyl chloride in the presence of pyridine. The resulting compounds were further cyclization converted to compound **35** that has a terminal chloroethyl group attached to the imidazole-fused ring. Treating compound **35** with various amines in DIPEA/THF gave the desired compounds **36**–**40** through nucleophilic substitution of the chlorine atom by appropriately substituted piperazine. The ^{13}C NMR data showed that the signal for carbonyl group on the core structure of anthraquinone was at the range δ 182–185 ppm whereas the signal of imidazole ring was at δ 154–161 ppm, respectively. Besides, all the final products were monitored by TLC; the quantities of the byproducts were separated from their physical chemistry properties and purification by tedious recrystallization and chromatography. All of the structural compounds were determined by ^{1}H NMR, ^{13}C NMR and high resolution mass (HRMS) spectra and the results are presented in the experimental part.

3. *In vitro* anti-proliferative activities

As reported in previous sections, all of the newly synthesized compounds were evaluated for their effects on cell viability in H1299 cell (Table 1). We found that most of the tested compounds showed cytotoxicity toward H1299 cells at micromolar ranges.

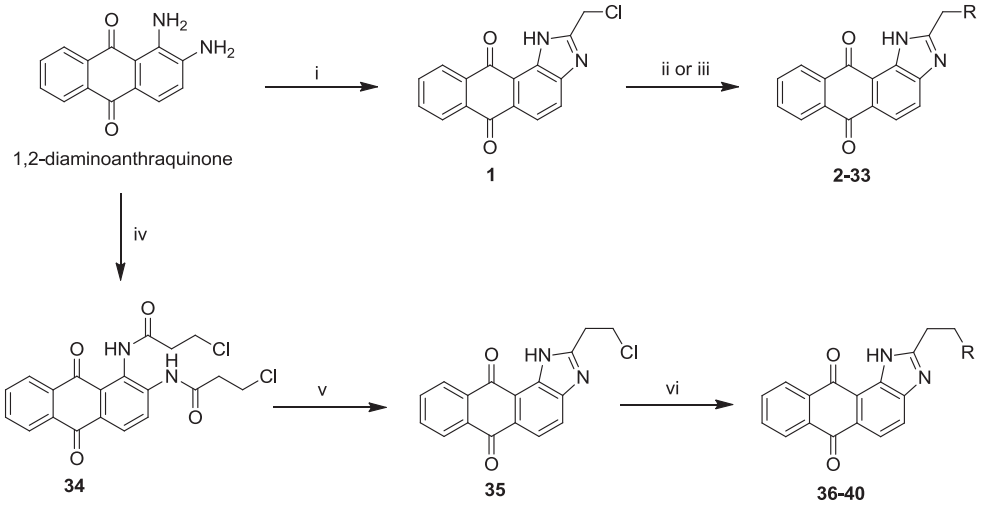

[a]Reagents and conditions: (i) chloroacetyl chloride, DMF, 80 °C, 8 hr. (ii) various amine, TEA, THF, reflux, 8 hr. (iii) various amine, DIPEA, THF, reflux, 6 hr. (iv) chloropropionyl chloride, pyridine, DMF, r.t., 24 hr. (v) 50% $H_2SO_{4\,(aq)}$, 110 °C, 2 hr, mini reactor. (vi) various amine, DIPEA, THF, reflux, 6 hr.

Scheme 2. [a]Synthesis of anthra[1,2-*d*]imidazole-6,11-dione derivatives **1**–**40**.

Among them, compounds **1**, **6**, **10**, **14**, and **20** showed strong cytotoxic effects toward H1299 cells. The anti-proliferation effects of these compounds were further analyzed using a PC-3 cancer cell line. The results were summarized in Table 2 and expressed as the amount of compounds required to achieve 50% growth inhibition (IC_{50}). These compounds showed IC_{50} values ranging from several micromolars to weak inhibitory effect with the maximum 30 μM concentration tested in our assays. It appeared that small side-chain extension might have better cytotoxic effects toward PC-3 cell. Among them, compounds **1**–**10**, **14**–**16**, **18**–**26**, **29**–**32**, **35**, **36** and **40** showed moderate potency against PC-3 with IC_{50} from 5.1 μM to 27.9 μM, respectively. With the exception of compounds **22** and **35** that showed preferential cytotoxic effects toward PC-3 cells, most of these compounds showed similar cytotoxic profiles toward H1299 and PC-3 cells. These compounds were also submitted to National Cancer Institute for 60 cell line drug screen program. Compounds **4** (NSC749234), **7** (NSC749238), **16** (NSC749236), **24** (NSC749235), **27** (NSC749237) and **28** (NSC749765) were selected to evaluate the cytotoxic effects toward 60 cell lines at a single dose of 10 μM (Table 3). These compounds exhibited preferential growth inhibition effects toward leukemia cell lines. Compounds **4**, **7**, and **24** showed less than 50% survival for more than half of the leukemia cell lines. Interestingly, compounds **4** and **24** might also have preference toward renal and colon cancers, respectively.

4. Telomerase inhibition and *hTERT* repression activities

The inhibitory effects of our synthesized imidazole-fused compounds on telomerase activities were also analyzed using the cell free extracts prepared from H1299 cells. We first tested the inhibitory activity of compounds **1**–**40** and the starting material 1,2-diaminoanthraquinone at 100 μM concentration (data not shown). Among them, only compounds **20**, **24**, and **25** showed significant telomerase inhibition activities. We next analyzed the concentration effects of compounds **20**, **24** and **25** against telomerase (Fig. 1). We found compound **20** showed potent telomerase inhibition activity with IC_{50} at ~5 μM. Compounds **24** and **25** were less effective with $IC_{50} > 10$ μM. Since TRAP assay involves both telomerase extension and PCR amplification steps, the effect of these compounds on Taq polymerase was also analyzed. Compounds **20**, **24** and **25** were added after the telomerase extension step during the TRAP assays (Fig. 1, TRAP-m). All three compounds did not show any detectable inhibitory activity in TRAP-m assays, suggesting that the inhibitory effect observed for these three compounds were due to the inhibition of telomerase activity. Thus, our results show that all three compounds specifically inhibited telomerase activity. Compound **20** is the most potent inhibitor among these compounds.

The catalytic subunit of telomerase *hTERT* expression was shown to be the key determining factor for telomerase activation in telomerase-positive cancer cells [31,32]. Herein, we also evaluated the *hTERT* repressing activity of our newly synthesized compounds by using a reporter assay that fused a SEAP reporter gene under the control of *hTERT* promoter. The expression of *hTERT* promoter-driven SEAP in H1299 cells was used as the criteria to determine the *hTERT* repressing activities of our new anthraquinone derivatives. Results of all tested compounds that showed SEAP inhibition activity at 1, 10 and 100 μM were summarized in Table 1. We have also determined the cell viability of the drug-treated H1299 cells in parallel using MTT assay. Significantly, quite a numbers of our compounds showed selective inhibitory effects on *hTERT* expression. Among these compounds, we were most interested in compounds **16**, **39**, and **40** because they affected the SEAP expression without significantly affecting the proliferation of the treated H1299 cells (Fig. 2). Thus, these compounds might selectively repress *hTERT* expression. The cytotoxic effects of these three compounds toward normal human diploid fibroblast IMR90 were also determined. All three compounds showed IC_{50} at ~100 μM toward IMR90, suggesting that they did not affect the general growth of normal cells (data not shown). Compound **40** appeared to show the best selectivity toward repressing *hTERT* expression. Interestingly, since a higher fraction of these compounds with long side chain (compounds **36** and **38**–**40**) showed selective *hTERT* repressing activities, the results suggested that the side chain length might play an important role in determining the *hTERT* repressing activity.

Table 1
Effects of anthra[1,2-*d*]imidazole-6,11-dione derivatives on cytotoxicity by MTT assay and repressing *hTERT* expression activity by SEAP assay.

Compounds	−R	Cell type/H1299					
		MTT assay (viability % ± SD)[a]			SEAP activity (% ± SD)[a]		
		1 (μM)	10 (μM)	100 (μM)	1 (μM)	10 (μM)	100 (μM)
1,2-diaminoanthraquinone		105 ± 9	95 ± 4	39 ± 9	99 ± 12	77 ± 12	18 ± 4
1	−Cl	82 ± 6	0 ± 2	0 ± 1	69 ± 2	0 ± 1	3 ± 1
2	$-N(CH_3)_2$	99 ± 6	64 ± 3	0 ± 2	84 ± 9	45 ± 1	0 ± 1
3	$-N(CH_3)(CH_2CH_3)$	99 ± 4	65 ± 3	0 ± 0	97 ± 12	39 ± 0	0 ± 1
4	$-N(CH_2CH_3)(CH_2CH_3)$	101 ± 7	55 ± 4	0 ± 0	91 ± 4	32 ± 4	0 ± 0
5	$-N(CH_3)(CH_2CH_2CH_3)$	93 ± 7	80 ± 4	0 ± 1	96 ± 7	34 ± 4	0 ± 1
6	$-N(CH_3)(CH(CH_3)_2)$	96 ± 5	23 ± 3	0 ± 1	77 ± 3	1 ± 1	0 ± 2
7	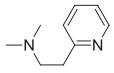	104 ± 1	99 ± 7	0 ± 1	96 ± 6	51 ± 2	0 ± 1
8	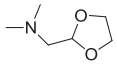	104 ± 4	90 ± 2	28 ± 1	90 ± 3	69 ± 2	7 ± 1
9	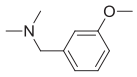	97 ± 5	98 ± 2	9 ± 5	105 ± 3	78 ± 2	0 ± 2
10	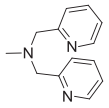	101 ± 6	13 ± 2	0 ± 2	86 ± 4	0 ± 1	0 ± 2
11	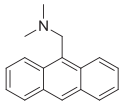	98 ± 4	84 ± 6	42 ± 7	102 ± 6	77 ± 6	12 ± 2
12	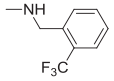	99 ± 5	96 ± 6	6 ± 2	87 ± 3	81 ± 7	0 ± 0
13	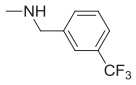	114 ± 3	110 ± 1	32 ± 2	87 ± 2	89 ± 2	4 ± 1
14	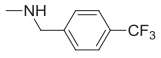	74 ± 4	11 ± 2	0 ± 1	52 ± 1	8 ± 7	2 ± 1
15	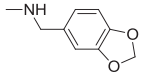	109 ± 2	103 ± 4	14 ± 3	75 ± 14	75 ± 17	1 ± 1
16		111 ± 9	79 ± 6	20 ± 3	76 ± 27	44 ± 16	7 ± 3
17	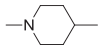	114 ± 3	110 ± 1	32 ± 3	102 ± 5	97 ± 5	26 ± 5
18		104 ± 7	85 ± 1	0 ± 1	107 ± 5	66 ± 4	4 ± 0
19	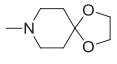	103 ± 2	79 ± 6	15 ± 3	97 ± 2	96 ± 1	14 ± 2
20	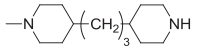	97 ± 5	0 ± 0	0 ± 1	96 ± 5	8 ± 0	3 ± 0
21		90 ± 3	71 ± 4	13 ± 6	102 ± 5	97 ± 5	26 ± 5
22		92 ± 4	77 ± 4	1 ± 1	115 ± 2	77 ± 2	5 ± 1
23		89 ± 5	76 ± 7	5 ± 2	106 ± 3	86 ± 1	12 ± 1
24	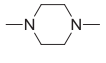	87 ± 6	35 ± 4	0 ± 1	106 ± 3	23 ± 1	6 ± 1
25	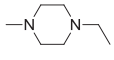	86 ± 5	35 ± 4	0 ± 1	92 ± 3	14 ± 1	0 ± 1

Table 1 (*continued*)

Compounds	−R	Cell type/H1299					
		MTT assay (viability % ± SD)[a]			SEAP activity (% ± SD)[a]		
		1 (μM)	10 (μM)	100 (μM)	1 (μM)	10 (μM)	100 (μM)
26	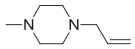	86 ± 3	45 ± 4	0 ± 1	87 ± 2	17 ± 4	0 ± 1
27	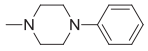	90 ± 4	54 ± 4	18 ± 4	92 ± 1	77 ± 6	6 ± 4
28	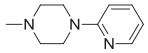	91 ± 4	69 ± 4	20 ± 2	91 ± 3	57 ± 1	1 ± 1
29	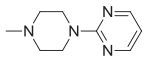	85 ± 3	74 ± 2	28 ± 2	111 ± 4	92 ± 3	19 ± 2
30	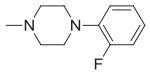	88 ± 2	77 ± 2	15 ± 2	103 ± 3	78 ± 4	0 ± 1
31	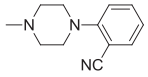	78 ± 5	62 ± 6	22 ± 1	106 ± 5	57 ± 8	6 ± 1
32	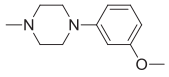	81 ± 10	58 ± 7	24 ± 3	105 ± 6	30 ± 7	3 ± 0
33	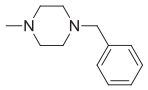	93 ± 2	51 ± 8	13 ± 3	98 ± 7	11 ± 1	0 ± 0
34	−	94 ± 3	34 ± 5	6 ± 2	87 ± 5	13 ± 4	0 ± 1
35	$-CH_2Cl$	91 ± 6	86 ± 3	40 ± 1	95 ± 9	83 ± 5	8 ± 4
36		87 ± 7	32 ± 6	0 ± 0	74 ± 3	7 ± 5	0 ± 1
37	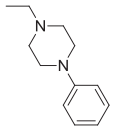	94 ± 1	96 ± 14	65 ± 9	103 ± 5	93 ± 5	37 ± 2
38	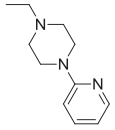	98 ± 8	93 ± 8	57 ± 11	88 ± 9	63 ± 3	1 ± 3
39	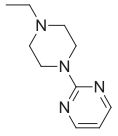	91 ± 6	84 ± 8	0 ± 2	83 ± 4	35 ± 3	0 ± 1
40	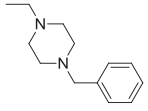	96 ± 8	54 ± 9	6 ± 3	73 ± 8	5 ± 5	0 ± 0

[a] SD: standard derivation, all experiments were independently performed at least three times.

5. Discussion and conclusion

In the course of our continuing search for new anticancer agents from anthraquinone moiety, we described an efficient synthesis and biological evaluation of a new series of rigid analogs of anthra [1,2-*d*]imidazole-6,11-dione. In this investigation, we focused our attention on the role of our systemic synthesized anthra[1,2-*d*] imidazole-6,11-dione as core pharmacophore bearing the imidazole moiety linked to the side chain. Forty new compounds have been designed and prepared, among which ten displayed cytotoxicity (IC_{50}) below 10 μM range toward PC-3 cells (Table 2). Evaluation of the antiproliferative activity against PC-3 human prostate cancer cells showed that the addition of small-sized functional groups to the imidazole ring enhanced the cell growth inhibition activities of these compounds. The NCI's 60 human cancer cell lines screen for compounds **4**, **7**, **16**, **24**, **27** and **28** revealed that most of the synthesized compounds moderately inhibited the growth of all cancer cell lines examined. Compound **24** appears to be the most active member of these compounds, suggesting that the methylpiperazine moiety of compound **24** might have a role its cytotoxic effects. While the mechanism of how these compounds rendered their cytotoxic activities is not fully

Table 2
Effects of compounds **1**–**40** on cytotoxicity of against the growth of PC-3 cells by SRB assay.

Cell type/PC-3 (Inhibition μM)[a]			
Compounds	IC_{50}	Compounds	IC_{50}
1	5.1	**22**	6.7
2	8.8	**23**	12.1
3	7.5	**24**	6.5
4	10.3	**25**	6.5
5	17.1	**26**	12.8
6	6.7	**27**	>30
7	14.2	**28**	>30
8	21	**29**	27.9
9	18.7	**30**	16.7
10	6.4	**31**	29
11	>30	**32**	15.3
12	>30	**33**	>30
13	>30	**34**	>30
14	7.6	**35**	5.2
15	22.5	**36**	17.3
16	10.3	**37**	>30
17	>30	**38**	>30
18	10.5	**39**	>30
19	21.6	**40**	16.0
20	13.8	–	–
21	12.4	–	–

[a] IC_{50} is the concentration of drug (μM) required to inhibit cell growth by 50% of the mean ($N = 3$).

clear to us, the information is valuable for future development of these compounds into anti-cancer therapies.

Of the series of compounds analyzed, we found compounds **20**, **24** and **25** exhibited telomerase inhibitory activity. In principle, telomerase inhibition should not lead to acute cell cytotoxicity. A long lag between telomerase inhibition and detrimental cellular effects is anticipated. For example, inhibition of telomerase activity using anti-sense peptide nucleic acid or 2′-*O*-MeRNA oligomers led to progressive telomere shortening and only caused cellular response after weeks of treatments [33]. Thus, the cytotoxic effects of H1299 cells by compounds **20**, **24** and **25** should not be simply due to their telomerase inhibition activities. The mechanism of how these compounds cause cytotoxic effects is not clear to us. However, since the anthracycline compounds were also known to inhibit topoisomerase activity and might inhibit telomerase activities through the stabilization of G-quadruplex structure formed by human G-rich DNA sequences, it is likely that these compounds cause cytotoxic effects through these mechanisms.

Table 3
Cytotoxicity of selected compounds in NCI's drug screen program.

Panel/cell lines	Compounds/growth percent[a] (at 10 μM)					
	4	**7**	**16**	**24**	**27**	**28**
Leukemia						
CCRF-CEM	47.88	39.91	102.47	34.45	74.42	–[b]
HL-60(TB)	68.18	120.08	56.89	65.29	107.54	97.31
MOLT-4	−9.43	47.54	22.77	−13.44	55.21	61.76
SR	42.38	70.10	57.64	21.48	43.11	–
K562	–	–	–	–	–	83.48
Non-small cell lung cancer						
EKVX	73.22	82.24	77.14	65.93	88.70	63.00
HOP-62	85.27	105.37	92.69	60.84	98.40	103.18
HOP-92	56.11	101.41	80.97	9.17	178.61	93.87
NCI-H226	77.20	81.36	78.85	64.48	82.98	91.88
NCI-H23	75.96	90.81	81.32	72.97	92.11	81.65
NCI-H322M	90.06	102.29	92.47	82.41	91.96	93.77
NCI-H460	55.50	90.27	64.61	57.35	94.45	79.98
NCI-H522	73.14	86.39	84.14	64.61	73.61	94.06
A549/ATCC	–	106.30	–	–	111.76	91.07
Colon cancer						
COLO 205	81.00	117.88	74.65	53.66	128.37	110.79
HCC-2998	80.61	95.82	82.81	61.90	–	92.28
HCT-116	48.22	83.56	62.12	27.73	78.28	84.30
HCT-15	65.75	80.78	54.20	44.98	74.39	86.02
HT29	56.02	84.18	61.38	22.64	87.57	75.79
KM12	76.89	89.03	77.40	55.51	85.80	95.03
SW-620	60.46	100.52	71.72	44.22	90.92	85.97
CNS cancer						
SF-268	74.04	85.87	58.46	51.16	80.44	79.15
SF-295	89.56	105.86	–	81.61	105.37	92.70
SF-539	85.26	102.32	82.47	63.88	112.36	104.29
SNB-19	75.06	87.77	76.33	65.60	103.62	81.00
SNB-75	82.03	81.62	86.42	69.87	70.93	82.14
U251	70.77	81.83	72.67	65.41	84.83	86.28
Melanoma						
LOX IMVI	61.98	89.67	62.99	43.47	95.76	82.25
MALME-3M	98.45	107.00	119.68	89.63	119.09	124.77
M14	97.86	106.97	100.82	97.20	106.33	103.99
MDA-MB-435	88.53	93.53	102.02	86.53	101.37	94.85
SK-MEL-2	102.69	95.03	113.29	107.95	101.39	98.34
SK-MEL-28	92.41	97.01	107.08	96.38	127.46	114.23
SK-MEL-5	68.20	75.48	65.73	77.46	74.84	83.56
UACC-62	68.47	89.67	74.61	81.12	93.36	85.13
UACC-257	–	–	–	–	–	88.91
Ovarian cancer						
IGROV1	13.61	54.26	54.22	12.05	69.25	91.25
OVCAR-3	63.32	83.57	66.26	52.79	76.56	88.67
OVCAR-4	65.69	80.99	65.27	50.98	67.72	64.57
OVCAR-5	96.50	109.14	101.70	97.72	107.63	110.77
OVCAR-8	–	80.59	–	–	80.89	88.07
NCI/ADR-RES	65.32	86.11	73.52	62.93	80.36	81.16
SK–OV-3	86.81	106.7	92.54	74.33	98.95	93.16
Renal cancer						
786–0	64.88	89.74	62.88	59.13	88.48	91.03
A489	49.50	69.60	61.84	69.36	75.09	68.23
ACHN	48.41	80.20	47.11	33.08	86.32	80.61
SN12C	69.04	91.19	96.96	48.50	89.91	79.85
TK-10	98.12	130.74	115.68	73.05	118.37	120.65
UO-31	27.21	49.49	42.93	22.93	58.33	60.42
CAKI-1	–	–	–	–	–	68.83
RXF 393	–	–	–	–	–	89.67
Prostate cancer						
PC-3	73.54	83.70	74.90	60.08	90.69	81.46
DU-145	–	99.83	81.94	–	77.91	89.10
Breast cancer						
MCF7	51.13	69.06	42.74	36.71	66.08	81.99
MDA-MB-231/	75.52	88.98	77.93	61.66	90.47	72.65
AHS 578-T	70.37	108.96	50.98	51.48	80.56	111.04
BT-549	105.50	114.38	109.47	100.53	110.22	102.42
T-47D	83.55	68.45	69.11	97.08	66.35	56.78
MDA-MB-468	54.46	77.09	58.32	71.59	72.75	53.92
Mean	69.66	89.07	75.35	59.85	90.15	87.65
Delta	79.09	49.16	52.58	73.29	47.04	33.73
Range	114.93	90.83	96.91	121.39	135.50	70.85

[a] Data obtained from NCI *in vitro* 60-cell line Program at 10 μM.
[b] Not test: (–).

Compounds **16**, **39**, and **40** were identified to repress *hTERT* expressions in H1299 cells. We consider the *hTERT* repressing effects of these compounds are specific as the same amounts of these compounds did not show equivalent level of cytotoxic effects. These compounds might repress *hTERT* expression directly through stabilizing the G-quadruplex structure located within the *hTERT* promoter. It is also likely that they might stabilize the G-quadruplex structure located within the *c-myc* promoter to indirectly repress *hTERT* expression. The detailed mechanism of how these compounds affect *hTERT* expression remains to be characterized. SARs analysis also revealed that the piperazine linker with a one- or two-carbon spacer between imidazole and amine might be an important functional moiety for *hTERT* repression or telomerase inhibition.

The cellular activities of the anthra[1,2-*d*]imidazole-6,11-dione derivatives appear to be greatly affected by its imidazole ring and various substituents on the core structure. We did not find apparent

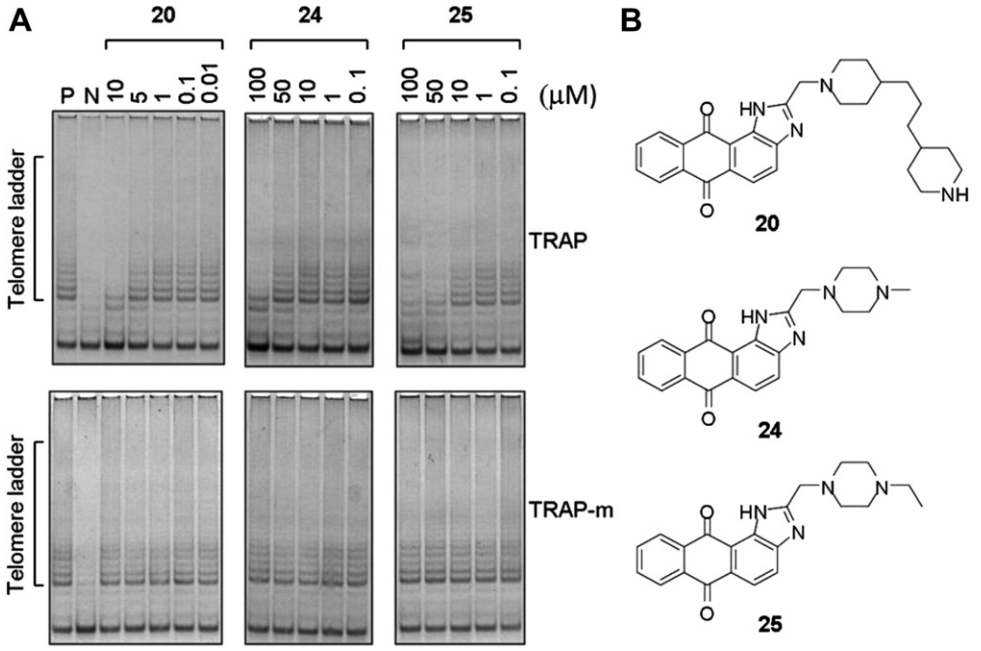

Fig. 1. Structures and the effects of compounds **20**, **24**, and **25** on telomerase activities. (A) In standard TRAP assays (top panels), indicated amounts of compounds were incubated with telomerase-active cell extracts for 5 min at room temperature before the telomerase-extension and PCR-amplification reactions. Telomerase-active cell extracts were prepared from H1299 cells (P) and the RNase A-treated extracts were used as negative controls (N). In TRAP-m assays (bottom panels), indicated amounts of the compounds were added right after the telomerase extension step and before the PCR-amplification step. (B) Structure of compounds **20**, **24**, and **25**.

correlation among telomerase inhibition, *hTERT* repression, and anti-proliferation of these compounds. Nevertheless, our analysis indicates that the imidazole-fused chromophore is a novel lead for anti-cancer therapies. Our analysis also provides further insight into designing the lead compounds for future drug development.

6. Materials and methods

6.1. Chemistry

Melting points were determined on a Büchi 545 melting point apparatus and are uncorrected. All reactions were monitored by TLC, which were performed on Silica Gel F_{254} plates (Merck). ^{1}H NMR and ^{13}C NMR spectra were recorded with a Varian GEMINI-300 (300 MHz) or Agilent 400 MR DD2 (400 MHz). Mass spectra were obtained on Finnigan MAT 95 XL HRMS and MAT 95 MS HRMS. These compounds were synthesized, starting from 1,2-diaminoanthraquinone and this starting material was purchased from Aldrich Chemical (Milwaukee, WI, USA). Reagents and solvents were purchased from Merck and Aldrich used without further purification.

6.2. General synthetic methods

6.2.1. General procedure (I): preparation of compound *1*

To a solution of 1,2-diaminoanthraquinone (1.19 g, 5 mmol) in DMF 20 mL was added chloroacetyl chloride (0.5 mL, 6 mmol) dropwise with stirring. The reaction mixture was stirred at 80 °C for

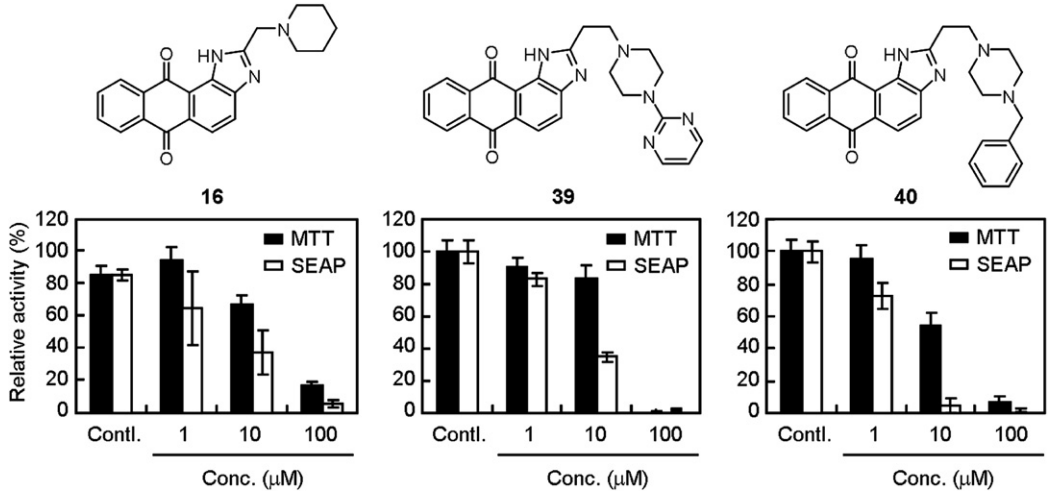

Fig. 2. Structures and the inhibition of P_{hTERT}-SEAP by compounds **16**, **39**, and **40**. About 2×10^3 cells of H1299 harboring P_{hTERT}-SEAP were seeded in 96-well plates and incubated at 37 °C for 24 h. Cells were then washed with PBS, re-cultured in fresh media, and incubated with varying amounts of compounds **16**, **39**, and **40** for another 48 h. The culture media were collected and subjected to SEAP activity analysis. The level of cell growth was also determined using MTT assay. The values are obtained from three experiments using the values without drug treatment as 100%.

10 h, and then poured into ice water (200 mL). The precipitate was collected on a filter, washed with ethanol.

*6.2.2. General procedure (II): preparation of compounds **2**–**15***

To a solution of compound **1** (1.18 g, 4 mmol) in THF 30 mL was added TEA (1.1 mL, 8 mmol) and series amine (8 mmol) dropwise with stirring. The reaction mixture was refluxed for 6 h. The mixture was concentrated and extracted with ethyl acetate, dried over $MgSO_4$, and the solvent was removed in vacuo. The formed precipitate was filtered off and dried in vacuo. Recrystallization from hexane and ethyl acetate, washed with acetone.

*6.2.3. General procedure (III): preparation of compounds **16**–**33***

To a solution of compound **1** (1.18 g, 4 mmol) in THF 30 mL was added DIPEA (1.4 mL, 8 mmol) and series amine (8 mmol) dropwise with stirring. The reaction mixture was refluxed for 8 h. The mixture was concentrated and extracted with ethyl acetate, dried over $MgSO_4$, and the solvent was removed in vacuo. The formed precipitate was filtered off and dried in vacuo. Recrystallization from hexane and ethyl acetate, washed with acetone.

*6.2.4. General procedure (IV): preparation of compound **34***

To a solution of 1,2-diaminoanthraquinone (0.95 g, 4 mmol) in DMF 30 mL was added pyridine (0.5 mL) and 3-chloropropionyl chloride (1.2 mL, 12 mmol) dropwise with stirring in ice-bath. The reaction mixture was stirred at room temperature under nitrogen for 24 h, and then poured into ice water (200 mL). The resulting precipitate was collected and purified by crystallization from hot ethanol.

*6.2.5. General procedure (V): preparation of compound **35***

Compound **34** (2.10 g, 5 mmol) was added to a 50% H_2SO_4 solution (10 mL) at 0 °C, and the reaction mixture was then heated at 110 °C for 2 h in mini-reactor. After cooling, the reaction mixture was extracted with dichloromethane, dried over $MgSO_4$, and the solvent was removed in vacuo. The formed precipitate was filtered off and dried in vacuo, washed with acetone.

*6.2.6. General procedure (VI): preparation of compounds **36**–**40***

To a solution of compound **35** (1.24 g, 4 mmol) in THF 30 mL was added DIPEA (1.4 mL, 8 mmol) and series amine (8 mmol) dropwise with stirring. The reaction mixture was refluxed for 6 h under nitrogen. The mixture was concentrated and extracted with ethyl acetate, dried over $MgSO_4$, and the solvent was removed in vacuo. The formed precipitate was filtered off and dried in vacuo. Recrystallization from hexane and ethyl acetate, washed with acetone.

*6.2.7. 2-(Chloromethyl)-1H-anthra[1,2-d]imidazole-6,11-dione (**1**)*

The pure compound was obtained as yellow powder (yield 65%). Mp 272–273 °C [13]. ^{1}H NMR (300 MHz, $CDCl_3$): δ ppm 4.92 (s, 2H), 7.80–7.83 (m, 2H), 8.08 (d, J = 8.4 Hz, 1H), 8.24 (d, J = 8.4 Hz, 1H), 8.26–8.35 (m, 2H), 11.21 (br, 1H). ^{13}C NMR (75 MHz, $CDCl_3$): δ ppm 37.80, 119.35, 121.27, 125.95, 126.83, 127.40, 129.06, 132.35, 133.47, 133.64, 134.88, 135.10, 148.89, 156.93, 183.04, 183.83. HRMS (EI) m/z: calcd for $[M]^+$: 296.0353, found: 296.0344.

*6.2.8. 2-((Dimethylamino)methyl)-1H-anthra[1,2-d]imidazole-6,11-dione (**2**)*

The pure compound was obtained as yellow powder (yield 40%). Mp 171–172 °C. ^{1}H NMR (300 MHz, $CDCl_3$): δ ppm 2.53 (s, 6H), 4.02 (s, 2H), 7.76–7.80 (m, 2H), 7.95 (d, J = 8.4 Hz, 1H), 8.13 (d, J = 8.4 Hz, 1H), 8.18–8.32 (m, 2H). ^{13}C NMR (75 MHz, $CDCl_3$): δ ppm 44.94, 56.69, 117.86, 120.92, 124.98, 126.01, 126.98, 128.25, 131.93, 132.80, 133.23, 133.41, 133.74, 148.21, 156.80, 182.34, 184.08. HRMS (ESI) m/z calcd for $[M]^+$: 305.1164, found: 306.1264 $[M + H]^+$, 328.1803$[M + Na]^+$.

*6.2.9. 2-((Ethylmethylamino)methyl)-1H-anthra[1,2-d]imidazole-6,11-dione (**3**)*

The pure compound was obtained as yellow powder (yield 51%). Mp 160–161 °C. ^{1}H NMR (300 MHz, $CDCl_3$): δ ppm 1.16 (t, J = 7.2 Hz, 3H), 2.35 (s, 3H), 2.60 (q, J = 7.2 Hz, 2H), 3.89 (s, 2H), 7.77–7.80 (m, 2H), 8.01 (d, J = 8.4 Hz, 1H), 8.18 (d, J = 8.4 Hz, 1H), 8.19–8.32 (m, 2H). ^{13}C NMR (75 MHz, $CDCl_3$): δ ppm 12.36, 42.43, 52.00, 55.64, 118.26, 121.49, 125.50, 126.55, 127.62, 128.64, 132.50, 133.55, 133.77, 134.19, 134.32, 149.32, 159.72, 182.98, 185.07. HRMS (ESI) m/z calcd for $[M]^+$: 319.1321, found: 320.1423 $[M + H]^+$, 342.1245 $[M + Na]^+$.

*6.2.10. 2-((Diethylamino)methyl)-1H-anthra[1,2-d]imidazole-6,11-dione (**4**)*

The pure compound was obtained as yellow powder (yield 45%). Mp 159–160 °C. ^{1}H NMR (300 MHz, $CDCl_3$): δ ppm 1.12 (t, J = 7.2 Hz, 6H), 2.68 (q, J = 7.2 Hz, 4H), 3.97 (s, 2H), 7.78–7.81 (m, 2H), 8.02 (d, J = 8.4 Hz, 1H), 8.20 (d, J = 8.4 Hz, 1H), 8.25–8.34 (m, 2H). ^{13}C NMR (75 MHz, $CDCl_3$): δ ppm. 12.10, 48.40, 52.18, 118.26, 121.51, 125.40, 126.56, 127.64, 128.56, 132.37, 133.61, 133.79, 134.25, 134.33, 149.59, 160.80, 183.05, 185.14. HRMS (ESI) m/z calcd for $[M]^+$: 333.1477, found: 334.1580 $[M + H]^+$, 356.1407 $[M + Na]^+$.

*6.2.11. 2-((Methylpropylamino)methyl)-1H-anthra[1,2-d] imidazole-6,11-dione (**5**)*

The pure compound was obtained as yellow powder (yield 43%). Mp 141–142 °C. ^{1}H NMR (300 MHz, $CDCl_3$): δ ppm 0.97 (t, J = 7.4 Hz, 3H), 1.59–1.61 (m, 2H), 2.42 (s, 3H), 2.55 (t, J = 7.5 Hz, 2H), 3.98 (s, 2H), 7.76–7.79 (m, 2H), 7.99 (d, J = 8.4 Hz, 1H), 8.16 (d, J = 8.4 Hz, 1H), 8.24–8.31 (m, 2H). ^{13}C NMR (75 MHz, $CDCl_3$): δ ppm 11.54, 20.22, 42.64, 55.90, 59.87, 118.34, 121.49, 125.44, 126.60, 127.56, 128.67, 132.45, 133.46, 133.80, 134.04, 134.30, 149.06, 158.76, 182.98, 184.84. HRMS (ESI) m/z calcd for $[M]^+$: 333.1477, found: 334.1579 $[M + H]^+$, 356.1405 $[M + Na]^+$.

*6.2.12. 2-((Ethylisopropylamino)methyl)-1H-anthra[1,2-d] imidazole-6,11-dione (**6**)*

The pure compound was obtained as yellow powder (yield 47%). Mp 165–166 °C. ^{1}H NMR (300 MHz, $CDCl_3$): δ ppm 1.14 (d, J = 6.6 Hz, 6H), 2.32 (s, 3H), 2.96–3.04 (m, 1H), 3.93 (s, 2H), 7.75–7.83 (m, 2H), 8.01 (d, J = 8.4 Hz, 1H), 8.19 (d, J = 8.1 Hz, 1H), 8.17–8.33 (m, 2H). ^{13}C NMR (75 MHz, $CDCl_3$): δ ppm 18.04, 37.91, 51.99, 54.15, 118.26, 121.49, 125.41, 126.54, 127.62, 128.57, 132.45, 133.58, 133.79, 134.21, 134.32, 149.52, 160.61, 183.03, 185.12. HRMS (ESI) m/z calcd for $[M]^+$: 333.1477, found: 334.1578 $[M + H]^+$, 356.1402 $[M + Na]^+$.

*6.2.13. 2-((N-Methyl-2-(pyridin-2-yl)ethanamino)methyl)-1H-anthra[1,2-d]imidazole-6,11-dione (**7**)*

The pure compound was obtained as yellow powder (yield 48%). Mp 150–151 °C. ^{1}H NMR (300 MHz, $CDCl_3$): δ ppm 2.44 (s, 3H), 3.01–3.11 (m, 4H), 4.00 (s, 2H), 7.13–7.17 (m, 1H), 7.21 (d, J = 7.5 Hz, 1H), 7.61–7.67 (m, 1H), 7.76–7.80 (m, 2H), 7.99 (d, J = 8.4 Hz, 1H), 8.16 (d, J = 8.7 Hz, 1H), 8.25–8.32 (m, 2H), 8.63–8.65 (m, 1H). ^{13}C NMR (75 MHz, $CDCl_3$): δ ppm 36.17, 42.99, 55.51, 57.49, 118.34, 121.41, 121.44, 123.28, 125.37, 126.54, 127.54, 128.59, 132.56, 133.50, 133.77, 134.04, 134.26, 136.61, 149.08, 149.67, 159.35, 160.11, 183.06, 184.73. HRMS (EI) m/z calcd for $[M]^+$: 396.1586, found: 396.1584.

*6.2.14. 2-(((1,3-Dioxolan-2-yl)-N-methylmethanamino)methyl)-1H-anthra[1,2-d] imidazole-6,11-dione (**8**)*

The pure compound was obtained as yellow powder (yield 59%). Mp 161–162 °C. ^{1}H NMR (300 MHz, $CDCl_3$): δ ppm 2.56 (s, 3H), 2.79 (d, J = 4.2 Hz), 3.98–4.03 (m, 2H), 4.09 (s, 2H), 4.13–4.17 (m, 2H), 5.15 (t, J = 4.2 Hz, 1H), 7.77–7.80 (m, 2H), 8.02 (d, J = 8.4 Hz, 1H), 8.20 (d, J = 8.4 Hz, 1H), 8.26–8.34 (m, 2H). ^{13}C NMR (75 MHz, $CDCl_3$): δ ppm 44.50, 56.03, 59.41, 65.09, 102.96, 118.39, 121.36,

125.24, 126.50, 127.46, 128.50, 132.33, 133.48, 133.67, 133.98, 134.15, 149.20, 158.92, 183.03, 184.57. HRMS (EI) *m/z* calcd for $[M]^+$: 377.1376, found: 377.1395.

*6.2.15. 2-((3-Methoxy-N-methybenzylamino)methyl)-1H-anthra [1,2-d]imidazole-6,11-dione (**9**)*

The pure compound was obtained as yellow powder (yield 39%). Mp 150–151 °C. ^{1}H NMR (300 MHz, $CDCl_3$): δ ppm 2.41 (s, 3H), 3.68 (s, 2H), 3.86 (s, 3H), 3.95 (s, 2H), 6.80–6.83 (m, 1H), 6.99–7.02 (m, 2H), 7.27 (t, *J* = 8.4 Hz, 1H), 7.78–7.82 (m, 2H), 8.02 (d, *J* = 8.4 Hz, 1H), 8.19 (d, *J* = 8.4 Hz, 1H), 8.26–8.34 (m, 2H). ^{13}C NMR (75 MHz, CDCl3): δ ppm 43.22, 55.19, 55.26, 62.40, 113.62, 114.39, 118.30, 121.48, 121.53, 125.55, 126.59, 127.66, 128.75, 129.67, 132.61, 133.40, 133.58, 133.80, 134.22, 134.35, 149.17, 159.03, 160.23, 183.00, 185.04. HRMS (ESI) *m/z* calcd for $[M]^+$: 411.1583, found: 412.1701 $[M + H]^+$, 434.1519 $[M + Na]^+$.

*6.2.16. 2-((Di-(2-picolyl)amino)methyl)-1H-anthra[1,2-d] imidazole-6,11-dione (**10**)*

The pure compound was obtained as yellow powder (yield 45%). Mp 175–176 °C. ^{1}H NMR (300 MHz, $CDCl_3$): δ ppm 4.04 (s, 4H), 4.20 (s, 2H), 7.25–7.29 (m, 2H), 7.46 (d, *J* = 7.5 Hz, 2H), 7.67–7.73 (m, 2H), 7.78–7.81 (m, 2H), 8.03 (d, *J* = 8.4 Hz, 1H), 8.21 (d, *J* = 8.4 Hz, 1H), 8.31–8.39 (m, 2H), 8.85–8.87 (m, 2H). ^{13}C NMR (75 MHz, $CDCl_3$): δ ppm 51.87, 59.73, 118.92, 121.32, 122.71, 123.86, 125.02, 126.68, 127.43, 128.64, 132.61, 133.68, 134.02, 134.06, 137.25, 149.03, 149.26, 149.58, 158.07, 159.30, 183.315, 184.44. HRMS (EI) *m/z* calcd for $[M]^+$: 459.1695, found: 459.1700.

*6.2.17. 2-(((Anthracen-10-yl)-N-methylmethanamino)methyl)-1H-anthra[1,2-d] imidazole-6,11-dione (**11**)*

The pure compound was obtained as yellow powder (yield 66%). Mp 189–190 °C. ^{1}H NMR (300 MHz, $CDCl_3$): δ ppm 2.55 (s, 3H), 3.97 (s, 2H), 4.69 (s, 2H), 7.42–7.47 (m, 2H), 7.60–7.66 (m, 2H), 7.45 (d, *J* = 7.8 Hz, 2H), 7.73–7.76 (m, 2H), 7.85 (d, *J* = 8.4 Hz, 1H), 7.92 (d, *J* = 8.4 Hz, 2H), 8.07 (d, *J* = 8.1 Hz, 1H), 8.19–8.27 (m, 2H), 8.32 (s, 1H), 8.51 (d, *J* = 9.3 Hz, 2H). ^{13}C NMR (75 MHz, $CDCl_3$): δ ppm 43.60, 53.72, 54.42, 118.00, 121.27, 124.29, 125.09, 126.50, 126.55, 127.46, 128.24, 128.39, 129.25, 131.37, 131.46, 132.22, 133.38, 133.68, 133.93, 134.15, 148.78, 158.99, 182.59, 184.37. HRMS (EI) *m/z* calcd for $[M]^+$: 481.1790, found: 481.1790.

*6.2.18. 2-((2-(Trifluoromethyl)benzylamino)methyl)-1H-anthra [1,2-d]imidazole-6,11-dione (**12**)*

The pure compound was obtained as yellow powder (yield 33%). Mp 143–144 °C. ^{1}H NMR (300 MHz, $CDCl_3$): δ ppm 4.09 (s, 2H), 4.21 (s, 2H), 7.39 (t, *J* = 7.5 Hz, 1H), 7.57 (t, *J* = 7.5 Hz, 1H), 7.65–7.68 (m, 2H), 7.71–7.81 (m, 2H), 7.98 (d, *J* = 8.1 Hz, 1H), 8.13 (d, *J* = 8.1 Hz, 1H), 8.16–8.31 (m, 2H). ^{13}C NMR (75 MHz, $CDCl_3$): δ ppm 47.01, 50.11, 118.28, 121.57, 122.84, 125.48, 126.25, 126.33, 126.40, 126.48, 126.59, 127.59, 128.57, 128.65, 128.97, 130.86, 132.19, 132.39, 133.48, 133.77, 134.13, 134.33, 137.83, 149.19, 159.53, 182.93, 184.96. HRMS (EI) *m/z* calcd for $[M]^+$: 435.1195, found: 435.1189.

*6.2.19. 2-((3-(Trifluoromethyl)benzylamino)methyl)-1H-anthra [1,2-d]imidazole-6,11-dione (**13**)*

The pure compound was obtained as yellow powder (yield 38%). Mp 155–156 °C. ^{1}H NMR (300 MHz, $CDCl_3$): δ ppm 4.00 (s, 2H), 4.23 (s, 2H), 7.45–7.54 (m, 2H), 7.60 (d, *J* = 6.9 Hz, 1H), 7.66 (s, 1H), 7.82–7.85 (m, 2H), 8.04 (d, *J* = 8.4 Hz, 1H), 8.22 (d, *J* = 8.4 Hz, 1H), 8.26–8.36 (m, 2H). ^{13}C NMR (75 MHz, $CDCl_3$): δ ppm 46.98, 53.35, 118.27, 121.60, 122.38, 124.32, 124.37, 124.41, 124.46, 124.99, 125.04, 125.10, 125.14,125.50, 125.98, 126.59, 127.61, 128.69, 131.71, 132.40, 133.43, 133.82, 134.10, 134.38, 140.28, 149.03, 159.17, 182.92, 184.97. HRMS (EI) *m/z* calcd for $[M]^+$: 435.1195, found: 435.1190.

*6.2.20. 2-((4-(Trifluoromethyl)benzylamino)methyl)-1H-anthra [1,2-d]imidazole-6,11-dione (**14**)*

The pure compound was obtained as yellow powder (yield 40%). Mp 158–159 °C. ^{1}H NMR (300 MHz, $CDCl_3$): δ ppm 4.00 (s, 2H), 4.22 (s, 2H), 7.52 (d, *J* = 7.8 Hz, 2H), 7.60 (d, *J* = 8.1 Hz, 2H), 7.78–7.84 (m, 2H), 8.03 (d, *J* = 8.4 Hz, 1H), 8.21 (d, *J* = 8.1 Hz, 1H), 8.25–8.37 (m, 2H). ^{13}C NMR (75 MHz, $CDCl_3$): δ ppm 37.84, 46.96, 53.28, 118.61, 121.64, 121.98, 125.50, 125.63, 126.27, 126.69, 127.72, 128.60, 129.42, 132.76, 133.29, 133.85, 133.98, 134.43, 134.59, 148.41, 154.59, 182.79, 184.99. HRMS (ESI) *m/z* calcd for $[M]^+$: 435.1195, found: 436.1318 $[M + H]^+$, 458.1143 $[M + Na]^+$.

*6.2.21. 2-((Piperonylamino)methyl)-1H-anthra[1,2-d]imidazole-6,11-dione (**15**)*

The pure compound was obtained as yellow powder (yield 50%). Mp 166–167 °C. ^{1}H NMR (300 MHz, $CDCl_3$): δ ppm 3.83 (s, 2H), 4.18 (s, 2H), 5.92 (s, 2H), 6.74–7.94 (m, 2H), 6.89 (s, 1H), 7.78–7.80 (m, 2H), 8.00 (d, *J* = 8.1 Hz, 1H), 8.18 (d, *J* = 8.4 Hz, 1H), 8.24–8.33 (m, 2H). ^{13}C NMR (75 MHz, $CDCl_3$): δ ppm 46.74, 53.71, 101.03, 108.31, 108.81, 118.26, 121.55, 121.61, 125.44, 126.60, 127.62, 128.62, 132.42, 133.28, 133.52, 133.79, 134.17, 134.35, 147.10, 148.13, 149.23, 159.86, 182.98, 184.99. HRMS (EI) *m/z* calcd for $[M]^+$: 435.1219, found: 435.1218.

*6.2.22. 2-((Piperidin-1-yl)methyl)-1H-anthra[1,2-d]imidazole-6,11-dione (**16**)*

The pure compound was obtained as yellow powder (yield 58%). Mp 204–205 °C. ^{1}H NMR (300 MHz, $CDCl_3$): δ ppm 1.50–1.53 (m, 2H), 1.65–1.72 (m, 4H), 2.54 (t, *J* = 5.1 Hz, 4H), 3.86 (s, 2H), 7.79–7.82 (m, 2H), 8.04 (d, *J* = 8.4 Hz, 1H), 8.21 (d, *J* = 8.4 Hz, 1H), 8.27–8.36 (m, 2H). ^{13}C NMR (75 MHz, $CDCl_3$): δ ppm 23.66, 25.62, 54.98, 56.92, 118.44, 121.51, 125.51, 126.65, 127.59, 128.79, 132.61, 133.55, 133.82, 134.12, 134.32, 149.07, 158.11, 183.03, 184.92. HRMS (EI) *m/z* calcd for $[M]^+$: 345.1477, found: 345.1468.

*6.2.23. 2-((4-Methylpiperidin-1-yl)methyl)-1H-anthra[1,2-d] imidazole-6,11-dione (**17**)*

The pure compound was obtained as yellow powder (yield 63%). Mp 208–209 °C. ^{1}H NMR (300 MHz, $CDCl_3$): δ ppm 0.97 (d, *J* = 5.7 Hz, 3H), 1.36–1.43 (m, 3H), 1.68 (d, *J* = 9.9 Hz, 2H), 2.23 (t, *J* = 11.7 Hz, 2H), 2.91 (d, *J* = 11.7 Hz, 2H), 3.89 (s, 2H), 7.61–7.83 (m, 2H), 8.03 (d, *J* = 8.4 Hz, 1H), 8.20 (d, *J* = 8.4 Hz, 1H), 8.25–8.34 (m, 2H). ^{13}C NMR (75 MHz, $CDCl_3$): δ ppm 21.57, 30.33, 34.22, 54.54, 56.81, 118.35, 121.51, 125.53, 126.60, 127.64, 128.73, 132.61, 133.60, 133.80, 134.22, 134.33, 149.26, 159.03, 183.02, 185.09. HRMS (ESI) *m/z* calcd for $[M]^+$: 359.1634, found: 360.1742 $[M + H]^+$, 382.1562 $[M + Na]^+$.

*6.2.24. 2-((Azepan-1-yl)methyl)-1H-anthra[1,2-d]imidazole-6,11-dione (**18**)*

The pure compound was obtained as yellow powder (yield 53%). Mp 183–184 °C. ^{1}H NMR (300 MHz, $CDCl_3$): δ ppm 1.72–1.81 (m, 8H), 2.92 (t, *J* = 5.3 Hz, 4H), 4.19 (s, 2H), 7.77–7.80 (m, 2H), 8.00 (d, *J* = 8.4 Hz, 1H), 8.18 (d, *J* = 8.4 Hz, 1H), 8.27–8.33 (m, 2H). ^{13}C NMR (75 MHz, $CDCl_3$): δ ppm 26.81, 28.15, 56.33, 56.50, 118.16, 121.42, 125.37, 126.55, 127.54, 128.49, 132.37, 133.42, 133.76, 134.02, 134.28, 149.19, 159.78, 182.96, 184.96. HRMS (ESI) *m/z* calcd for $[M]^+$: 359.1634, found: 360.1746 $[M + H]^+$, 382.1559 $[M + Na]^+$.

*6.2.25. 2-((1,4-Dioxa-8-azaspiro[4.5]decane-8-yl)methyl)-1H-anthra[1,2-d]imidazole-6,11-dione (**19**)*

The pure compound was obtained as yellow powder (yield 60%). Mp 219–220 °C. ^{1}H NMR (300 MHz, $CDCl_3$): δ ppm 1.87 (t, *J* = 5.6 Hz, 4H), 2.78 (t, *J* = 5.4 Hz, 4H), 3.97 (s, 4H), 4.01 (s, 2H), 7.76–7.79 (m, 2H), 7.99 (d, *J* = 8.4 Hz, 1H), 8.16 (d, *J* = 8.4 Hz, 1H), 8.22–8.31 (m, 2H). ^{13}C NMR (75 MHz, $CDCl_3$): δ ppm 34.47, 51.92, 55.77, 64.37, 106.36, 118.48, 121.54, 125.57, 126.66, 127.57, 128.87,

132.60, 133.45, 133.85, 134.03, 134.33, 148.88, 182.97, 184.81. HRMS (EI) *m/z* calcd for $[M]^+$: 403.1532, found: 403.1530.

*6.2.26. 2-((4-(3-(Piperidin-4-yl)propyl)piperidin-1-yl)methyl)-1H-anthra[1,2-d] imidazole-6,11-dione (**20**)*

The pure compound was obtained as yellow powder (yield 40%). Mp 172–173 °C. ^{1}H NMR (300 MHz, $CDCl_3$): δ ppm 1.04–1.28 (m, 12H), 1.64–1.68 (m, 4H), 2.14–2.21 (m, 2H), 2.54–2.62 (m, 2H), 2.90 (d, *J* = 11.4 Hz, 2H), 3.07 (d, *J* = 12.3 Hz, 2H), 3.86 (s, 2H), 4.22 (br, 1H), 7.74–7.81 (m, 2H), 8.00 (d, *J* = 8.4 Hz, 1H), 8.17 (d, *J* = 8.4 Hz, 1H), 8.20–8.32 (m, 2H). ^{13}C NMR (75 MHz, $CDCl_3$): δ ppm 23.49, 32.34, 33.26, 35.29, 36.02, 36.56, 37.22, 46.53, 54.60, 56.86, 118.20, 121.44, 125.46, 126.52, 127.59, 128.57, 132.51, 133.44, 133.80, 134.05, 134.33, 149.10, 159.17, 182.99, 185.05. HRMS (EI) *m/z* calcd for $[M]^+$: 470.2682, found: 470.2689.

*6.2.27. 2-(Morpholinomethyl)-1H-anthra[1,2-d]imidazole-6,11-dione (**21**)*

The pure compound was obtained as yellow powder (yield 55%). Mp 241–242 °C. ^{1}H NMR (300 MHz, $CDCl_3$): δ ppm 2.64 (t, *J* = 4.5 Hz, 4H), 3.81 (t, *J* = 4.7 Hz, 4H), 3.93 (s, 2H), 7.76–7.80 (m, 2H), 8.00 (d, *J* = 8.4 Hz, 1H), 8.16 (d, *J* = 8.4 Hz, 1H), 8.21–8.31 (m, 2H). ^{13}C NMR (75 MHz, $CDCl_3$): δ ppm 53.90, 56.74, 66.72, 118.26, 121.57, 125.65, 126.54, 127.61, 128.77, 132.52, 133.35, 133.85, 134.00, 134.42, 148.84, 157.44, 182.87, 185.02. HRMS (ESI) *m/z* calcd for $[M]^+$: 347.1270, found: 348.1379 $[M + H]^+$, 370.1198 $[M + Na]^+$.

*6.2.28. 2-(Thiomorpholinomethyl)-1H-anthra[1,2-d]imidazole-6,11-dione (**22**)*

The pure compound was obtained as yellow powder (yield 59%). Mp 216–217 °C. ^{1}H NMR (300 MHz, $CDCl_3$): δ ppm 2.82 (t, *J* = 4.7 Hz, 4H), 2.96 (t, *J* = 4.8 Hz, 4H), 4.02 (s, 2H), 7.78–7.81 (m, 2H), 8.01 (d, *J* = 8.4 Hz, 1H), 8.18 (d, *J* = 8.7 Hz, 1H), 8.23–8.33 (m, 2H). ^{13}C NMR (75 MHz, $CDCl_3$): δ ppm 27.56, 55.32, 56.93, 118.45, 121.64, 125.67, 126.65, 127.64, 128.95, 132.59, 133.44, 133.89, 134.06, 134.42, 148.87, 156.97, 182.91, 184.96. HRMS (ESI) *m/z* calcd for $[M]^+$: 363.1041, found: 364.1141 $[M + H]^+$, 386.0907 $[M + Na]^+$.

*6.2.29. 2-((Thiazolidin-3-yl)methyl)-1H-anthra[1,2-d]imidazole-6,11-dione (**23**)*

The pure compound was obtained as yellow powder (yield 48%). Mp 195–196 °C. ^{1}H NMR (300 MHz, $CDCl_3$): δ ppm 3.10 (t, *J* = 6.5 Hz, 2H), 3.31 (t, *J* = 6.5 Hz, 2H), 4.13 (s, 2H), 4.24 (s, 2H), 7.79–7.83 (m, 2H), 8.01 (d, *J* = 8.4 Hz, 1H), 8.19 (d, *J* = 8.4 Hz, 1H), 8.23–8.35 (m, 2H). ^{13}C NMR (75 MHz, $CDCl_3$): δ ppm 29.47, 52.11, 58.09, 60.86, 118.41, 121.69, 125.79, 126.59, 127.69, 128.92, 132.60, 133.49, 133.86, 134.16, 134.45, 149.07, 158.11, 182.92, 185.12. HRMS (ESI) *m/z* calcd for $[M]^+$: 349.0885, found: 350.0999 $[M + H]^+$, 372.0816 $[M + Na]^+$.

6.2.30. 2-((4-Methylpiperazin-1-yl)methyl)-1H-anthra[1,2-d] imidazole-6,11-di-one (24)

The pure compound was obtained as yellow powder (yield 70%). Mp 231–232 °C. ^{1}H NMR (300 MHz, $CDCl_3$): δ ppm 2.37 (s, 3H), 2.61–2.69 (m, 8H), 3.92 (s, 2H), 7.76–7.79 (m, 2H), 8.00 (d, *J* = 8.4 Hz, 1H), 8.16 (d, *J* = 8.4 Hz, 1H), 8.22–8.32 (m, 2H). ^{13}C NMR (75 MHz, $CDCl_3$): δ ppm 45.64, 53.27, 54.85, 56.28, 118.26, 121.54, 125.66, 126.53, 127.63, 128.75, 132.55, 133.47, 133.80, 134.16, 134.38, 149.07, 158.18, 182.89, 185.10. HRMS (EI) *m/z* calcd for $[M]^+$: 360.1586, found: 360.1585.

*6.2.31. 2-((4-Ethylpiperazin-1-yl)methyl)-1H-anthra[1,2-d] imidazole-6,11-dione (**25**)*

The pure compound was obtained as yellow powder (yield 64%). Mp 204–205 °C. ^{1}H NMR (300 MHz, $CDCl_3$): δ ppm 1.09 (t, *J* = 7.2 Hz, 3H), 2.46 (q, *J* = 7.2 Hz, 2H), 2.58–2.67 (m, 8H), 3.91 (s, 2H), 7.75–7.77 (m, 2H), 7.99 (d, *J* = 8.4 Hz, 1H), 8.14 (d, *J* = 8.4 Hz, 1H), 8.19–8.29 (m, 2H). ^{13}C NMR (75 MHz, $CDCl_3$): δ ppm 11.75, 52.13, 52.55, 53.49, 56.35, 118.17, 121.48, 125.57, 126.49, 127.57, 128.62, 132.48, 133.36, 133.79, 134.00, 134.35, 148.97, 158.31, 182.88, 185.01. HRMS (EI) *m/z* calcd for $[M]^+$: 374.1743, found: 374.1736.

*6.2.32. 2-((4-Allylpiperazin-1-yl)methyl)-1H-anthra[1,2-d] imidazole-6,11-dione (**26**)*

The pure compound was obtained as yellow powder (yield 54%). Mp 175–176 °C. ^{1}H NMR (300 MHz, $CDCl_3$) δ ppm 2.81 (s, 8H), 3.22 (d, *J* = 6.6 Hz, 2H), 3.97 (s, 2H), 5.27–5.33 (m, 2H), 5.97 (m, 1H), 7.77–7.84 (m, 2H), 8.04 (d, *J* = 8.4 Hz, 1H), 8.21 (d, *J* = 8.7 Hz, 1H), 8.23–8.35 (m, 2H). ^{13}C NMR (75 MHz, $CDCl_3$): δ ppm 29.60, 52.37, 52.62, 56.10, 61.02, 118.34, 120.25, 121.64, 125.76, 126.57, 127.69, 128.86, 132.58, 133.46, 133.86, 134.13, 134.46, 149.03, 157.66, 182.93, 185.16. HRMS (EI) *m/z* calcd for $[M]^+$: 386.1743, found: 386.1734.

*6.2.33. 2-((4-Phenylpiperazin-1-yl)methyl)-1H-anthra[1,2-d] imidazole-6,11-di-one (**27**)*

The pure compound was obtained as yellow powder (yield 68%). Mp 212–213 °C. ^{1}H NMR (300 MHz, $CDCl_3$): δ ppm 2.82 (t, *J* = 4.8 Hz, 4H), 3.31 (t, *J* = 4.8 Hz, 4H), 4.02 (s, 2H), 6.88–6.95 (m, 3H), 7.24–7.30 (m, 2H), 7.76–7.79 (m, 2H), 8.07 (d, *J* = 8.7 Hz, 1H), 8.17 (d, *J* = 8.1 Hz, 1H), 8.20–8.31 (m, 2H). ^{13}C NMR (75 MHz, $CDCl_3$): δ ppm 49.06, 53.52, 56.30, 116.35, 118.28, 120.15, 121.54, 125.60, 126.54, 127.57, 128.74, 129.22, 132.52, 133.33, 133.84, 133.96, 134.38, 148.85, 151.12, 157.58, 182.88, 184.93. HRMS (EI) *m/z* calcd for $[M]^+$: 422.1743, found: 422.1744.

*6.2.34. 2-((4-(Pyridin-2-yl)piperazin-1-yl)methyl)-1H-anthra[1,2-d]imidazole-6,11-dione (**28**)*

The pure compound was obtained as yellow powder (yield 63%). Mp 200–201 °C. ^{1}H NMR (300 MHz, $CDCl_3$): δ ppm 2.80 (t, *J* = 4.8 Hz, 4H), 3.69 (t, *J* = 5.0 Hz, 4H), 4.04 (s, 2H), 6.64–6.68 (m, 2H), 7.48–7.51 (m, 1H), 7.77–7.80 (m, 2H), 8.03 (d, *J* = 8.4 Hz, 1H), 8.33–8.17 (m, 3H). ^{13}C NMR (75 MHz, $CDCl_3$): δ ppm 45.17, 53.36, 56.42, 107.23, 113.64, 118.34, 121.57, 125.64, 126.57, 127.60, 128.82, 132.58, 133.42, 133.83, 134.06, 134.38, 137.67, 148.00, 148.96, 157.66, 159.37, 182.90, 184.99. HRMS (EI) *m/z* calcd for $[M]^+$: 423.1695, found: 423.1694.

*6.2.35. 2-((4-(Pyrimidin-2-yl)piperazin-1-yl)methyl)-1H-anthra [1,2-d]imidazole-6,11-dione (**29**)*

The pure compound was obtained as yellow powder (yield 59%). Mp 223–224 °C. ^{1}H NMR (300 MHz, $CDCl_3$): δ ppm 2.70 (t, *J* = 5.0 Hz, 4H), 3.95 (t, *J* = 5.0 Hz, 4H), 3.99 (s, 2H), 6.51 (t, *J* = 4.8 Hz, 1H), 7.79–7.82 (m, 2H), 8.06 (d, *J* = 8.4 Hz, 1H), 8.22 (d, *J* = 8.7 Hz, 1H), 8.26–8.35 (m, 4H). ^{13}C NMR (75 MHz, $CDCl_3$): δ ppm. 43.58, 53.48, 56.56, 110.18, 118.34, 121.60, 125.69, 126.59, 127.65, 128.82, 132.61, 133.44, 133.87, 134.07, 134.43, 148.97, 157.85, 161.82, 182.96, 185.10. HRMS (EI) *m/z* calcd for $[M]^+$: 424.1648, found: 424.1652.

*6.2.36. 2-((4-(2-Fluorophenyl)piperazin-1-yl)methyl)-1H-anthra [1,2-d]imidazole-6,11-dione (**30**)*

The pure compound was obtained as yellow powder (yield 67%). Mp 163–164 °C. ^{1}H NMR (300 MHz, $CDCl_3$): δ ppm 2.89 (t, *J* = 4.4 Hz, 4H), 3.25 (t, *J* = 4.7 Hz, 4H), 4.08 (s, 2H), 6.94–7.07 (m, 4H), 7.77–7.80 (m, 2H), 8.03 (d, *J* = 8.4 Hz, 1H), 8.18 (d, *J* = 8.4 Hz, 1H), 8.23–8.33 (m, 4H). ^{13}C NMR (75 MHz, $CDCl_3$): δ ppm 50.17, 53.61, 56.23, 116.13, 116.40, 118.39, 119.21, 119.25, 121.59, 122.82, 122.92, 124.55, 124.60, 125.67, 126.59, 127.61, 128.85, 132.58, 133.41, 133.84, 134.03, 134.39, 139.74, 139.86, 148.90, 154.29, 157.56, 182.91, 184.96. HRMS (EI) *m/z* calcd for $[M]^+$: 440.1649, found: 440.1643.

*6.2.37. 2-((4-(2-Cyanophenyl)piperazin-1-yl)methyl)-1H-anthra[1,2-d]imidazole-6,11-dione (**31**)*

The pure compound was obtained as yellow powder (yield 45%). Mp 230–231 °C. ^{1}H NMR (300 MHz, $CDCl_3$): δ ppm 2.94 (t, J = 4.2 Hz, 4H), 3.37 (t, J = 4.7 Hz, 4H), 4.10 (s, 2H), 7.47–7.59 (m, 2H), 7.77–7.80 (m, 2H), 8.02 (d, J = 8.4 Hz, 1H), 8.18 (d, J = 8.4 Hz, 1H), 8.22–8.32 (m, 4H). ^{13}C NMR (75 MHz, $CDCl_3$): δ ppm 51.15, 53.53, 56.09, 106.59, 118.22, 118.48, 119.03, 121.67, 122.37, 125.81, 126.63, 127.67, 129.00, 132.65, 133.48, 133.87, 133.91, 134.12, 134.43, 134.47, 134.68, 148.94, 155.35, 182.93, 185.03. HRMS (EI) m/z calcd for $[M]^+$: 447.1695, found: 447.1712.

*6.2.38. 2-((4-(3-Methoxyphenyl)piperazin-1-yl)methyl)-1H-anthra[1,2-d]imidazole-6,11-dione (**32**)*

The pure compound was obtained as yellow powder (yield 58%). Mp 150–151 °C. ^{1}H NMR (300 MHz, $CDCl_3$): δ ppm 2.89 (s, 4H), 3.35 (t, J = 4.8 Hz, 4H), 3.79 (s, 3H), 4.13 (s, 2H), 6.43–6.56 (m, 3H), 7.18 (t, J = 8.1 Hz, 1H), 7.77–7.80 (m, 2H), 8.02 (d, J = 8.1 Hz, 1H), 8.19 (d, J = 8.4 Hz, 1H), 8.23–8.33 (m, 4H). ^{13}C NMR (75 MHz, $CDCl_3$): δ ppm 48.80, 53.36, 55.18, 56.09, 103.06, 105.21, 109.23, 118.51, 121.63, 125.68, 126.67, 127.61, 128.97, 129.99, 132.63, 133.42, 133.88, 134.03, 134.39, 148.80, 160.88, 182.94, 184.86. HRMS (EI) m/z calcd for $[M]^+$: 452.1848, found: 452.1846.

*6.2.39. 2-((4-Benzylpiperazin-1-yl)methyl)-1H-anthra[1,2-d]imidazole-6,11-dione (**33**)*

The pure compound was obtained as yellow powder (yield 62%). Mp 194–195 °C. ^{1}H NMR (300 MHz, $CDCl_3$): δ ppm 2.64–2.69 (m, 8H), 3.60 (s, 2H), 3.92 (s, 2H), 7.27–7.36 (m, 5H), 7.76–7.80 (m, 2H), 8.00 (d, J = 8.1 Hz, 1H), 8.16 (d, J = 8.4 Hz, 1H), 8.22–8.31 (m, 4H). ^{13}C NMR (75 MHz, $CDCl_3$): δ ppm. 52.84, 53.50, 56.32, 62.81, 118.17, 121.48, 125.55, 126.49, 127.27, 127.57, 128.34, 128.61, 129.26, 132.46, 133.36, 133.78, 134.00, 134.35, 137.78, 148.98, 158.34, 182.87, 185.00. HRMS (EI) m/z calcd for $[M]^+$: 436.1899, found: 436.1902.

*6.2.40. 1,2-Bis-(3-chloropropionamido)anthraquinone (**34**)*

The pure compound was obtained as yellow powder (yield 51%). Mp 179–180 °C [22]. ^{1}H NMR (300 MHz, DMSO-d_6): δ ppm 2.94–3.03 (m, 4H), 3.86–3.94 (m, 4H), 7.88–7.90 (m, 2H), 8.10–8.15 (m, 2H), 8.08 (d, J = 8.1 Hz, 1H), 8.42 (d, J = 8.7 Hz, 1H), 9.50 (s, 1H), 10.02 (s, 1H). ^{13}C NMR (75 MHz, DMSO-d_6): δ ppm. 40.20, 40.26, 125.94, 126.29, 126.87, 127.61, 127.79, 128.33, 129.79, 132.27, 134.26, 134.36, 134.52, 140.28, 168.86, 169.43, 181.63, 183.22. HRMS (EI) m/z calcd for $[M]^+$: 418.0487, found: 418.0494.

*6.2.41. 2-(2-Chloroethyl)-1H-anthra[1,2-d]imidazole-6,11-dione (**35**)*

The pure compound was obtained as yellow powder (yield 68%). Mp 261–262 °C. ^{1}H NMR (400 MHz, $CDCl_3$): δ ppm 3.53 (t, J = 6.4 Hz, 2H), 4.07 (t, J = 6.4 Hz, 2H), 7.79–7.85 (m, 2H), 8.09 (d, J = 8.4 Hz, 1H), 8.25 (d, J = 8.1 Hz, 1H), 8.26–8.36 (m, 2H). ^{13}C NMR (100 MHz, DMSO-d_6): δ ppm. 31.79, 42.13, 118.24, 120.52, 120.99, 124.32, 125.44, 126.22, 126.78, 127.70, 132.94, 133.10, 134.25, 134.48, 158.75, 182.41, 183.27. HRMS (EI) m/z calcd for $[M]^+$: 310.0509, found: 310.0511.

*6.2.42. 2-(2-(4-Methylpiperazin-1-yl)ethyl)-1H-anthra[1,2-d]imidazole-6,11-dione (**36**)*

The pure compound was obtained as yellow powder (yield 71%). Mp 190–191 °C. ^{1}H NMR (300 MHz, $CDCl_3$): δ ppm 2.54 (s, 3H), 2.70 (s, 4H), 2.89 (s, 4H), 2.93 (t, J = 6.0 Hz, 2H), 3.20 (t, J = 5.7 Hz, 2H), 7.75–7.78 (m, 2H), 7.96 (d, J = 8.4 Hz, 1H), 8.15 (d, J = 8.1 Hz, 1H), 8.16–8.31 (m, 2H). ^{13}C NMR (75 MHz, $CDCl_3$): δ ppm. 25.26, 45.79, 52.43, 54.74, 54.90, 118.17, 121.31, 124.91, 126.57, 127.49, 128.23, 132.35, 133.62, 134.13, 148.78, 160.55, 183.19, 184.48. HRMS (EI) m/z calcd for $[M]^+$: 374.1743, found: 374.1740.

*6.2.43. 2-(2-(4-Phenylpiperazin-1-yl)ethyl)-1H-anthra[1,2-d]imidazole-6,11-dione (**37**)*

The pure compound was obtained as yellow powder (yield 67%). Mp 211–212 °C. ^{1}H NMR (300 MHz, $CDCl_3$): δ ppm 2.95 (s, 4H), 3.09 (s, 2H), 3.33 (t, J = 5.6 Hz, 2H), 3.56 (t, J = 4.8 Hz, 4H), 6.93 (t, J = 7.4 Hz, 1H), 7.05 (d, J = 7.8 Hz, 2H), 7.31–7.37 (m, 2H), 7.73–7.77 (m, 2H), 7.93 (d, J = 8.4 Hz, 1H), 8.14 (d, J = 8.4 Hz, 1H), 8.18–8.31 (m, 2H). ^{13}C NMR (75 MHz, $CDCl_3$): δ ppm. 25.34, 49.22, 52.93, 55.07, 116.47, 117.39, 118.25, 120.02, 121.34, 124.89, 126.75, 127.43, 128.30, 129.30, 129.49, 132.39, 133.57, 133.65, 134.11, 148.77, 151.36, 183.19, 184.50. HRMS (EI) m/z calcd for $[M]^+$: 436.1899, found: 436.1896.

*6.2.44. 2-(2-(4-(Pyridin-2-yl)piperazin-1-yl)ethyl)-1H-anthra[1,2-d]imidazole-6,11-dione (**38**)*

The pure compound was obtained as yellow powder (yield 65%). Mp 234–235 °C. ^{1}H NMR (300 MHz, $CDCl_3$): δ ppm 2.87 (s, 4H), 3.02 (t, J = 5.3 Hz, 2H), 3.31 (t, J = 5.9 Hz, 2H), 3.93 (s, 4H), 6.69 (t, J = 6 Hz, 1H), 6.76 (d, J = 8.4 Hz, 1H), 7.53–7.58 (m, 1H), 7.73–7.77 (m, 2H), 7.99 (d, J = 8.4 Hz, 1H), 8.17 (d, J = 8.4 Hz, 1H), 8.22–8.32 (m, 3H). ^{13}C NMR (75 MHz, $CDCl_3$): δ ppm. 25.21, 45.05, 52.68, 55.10, 107.28, 113.63, 118.26, 121.37, 124.92, 126.76, 127.46, 128.32, 132.39, 133.54, 133.68, 134.07, 134.14, 137.80, 148.08, 148.72, 159.32, 160.07, 183.20, 184.51. HRMS (EI) m/z calcd for $[M]^+$: 437.1852, found: 437.1856.

*6.2.45. 2-(2-(4-(Pyrimidin-2-yl)piperazin-1-yl)ethyl)-1H-anthra[1,2-d]imidazole-6,11-dione (**39**)*

The pure compound was obtained as yellow powder (yield 61%). Mp 230–231 °C. ^{1}H NMR (300 MHz, $CDCl_3$): δ ppm 2.81 (s, 4H), 3.01 (t, J = 5.6 Hz, 2H), 3.30 (t, J = 5.6 Hz, 2H), 4.20 (s, 4H), 6.54 (t, J = 4.7 Hz, 1H), 7.73–7.76 (m, 2H), 7.97 (d, J = 8.4 Hz, 1H), 8.16 (d, J = 8.4 Hz, 1H), 8.22–8.31 (m, 2H), 8.36 (d, J = 4.8 Hz, 2H). ^{13}C NMR (75 MHz, $CDCl_3$): δ ppm. 25.20, 43.57, 52.77, 55.10, 110.15, 118.22, 121.34, 124.89, 126.72, 127.45, 128.27, 132.35, 133.55, 133.66, 134.06, 134.13, 148.71, 157.93, 160.27, 161.81, 183.19, 184.51. HRMS (EI) m/z calcd for $[M]^+$: 438.1804, found: 438.1806.

*6.2.46. 2-(2-(4-Benzylpiperazin-1-yl)ethyl)-1H-anthra[1,2-d]imidazole-6,11-dione (**40**)*

The pure compound was obtained as yellow powder (yield 51%). Mp 177–178 °C. ^{1}H NMR (300 MHz, $CDCl_3$): δ ppm 2.70 (s, 4H), 2.83 (s, 4H), 2.90 (t, J = 6.0 Hz, 2H), 3.19 (t, J = 6.0 Hz, 2H), 3.71 (s, 2H), 7.28–7.44 (m, 5H), 7.77–7.80 (m, 2H), 7.96 (d, J = 8.4 Hz, 1H), 8.15 (d, J = 8.4 Hz, 1H), 8.28–8.32 (m, 2H). ^{13}C NMR (75 MHz, $CDCl_3$): δ ppm. 25.22, 52.21, 52.61, 54.71, 62.68, 118.19, 121.32, 124.91, 126.59, 127.50, 127.68, 128.26, 128.55, 129.09, 129.66, 132.36, 133.58, 133.63, 134.11, 134.16, 148.75, 160.29, 183.16, 184.48. HRMS (EI) m/z calcd for $[M]^+$: 450.2056, found: 450.2050.

6.3. Cell cultures and assessment of hTERT

Non-small lung cancer cell H1299 was grown in RPMI 1640 media supplemented with 10% fetal bovine serum, 100 units/mL penicillin and 100 mg/mL streptomycin in a humidified atmosphere with 5% CO_2 at 37 °C. Culture media were changed every 3 days. To establish stable cell lines that the expression of *hTERT* could be monitored by a reporter system, a ~3.3 kbp DNA fragment ranging from −3338 to +1 bp of the *hTERT* gene was subcloned upstream to a SEAP gene and transfected into H1299 by electroporation. The stable clones were selected using G418. The stable clones derived from H1299 was cultured using conditions that are similar to their parental cells.

6.4. Telomere repeat amplification protocol (TRAP assay)

Telomerase activity was detected by modifying version of the TRAP protocol [27,28]. Telomerase products were resolved by 10%

polyacrylamide gel electrophoresis and visualized by staining with SYBER Green. As a source of telomerase, the total cell lysates derived from lung cancer cell line (H1299) was used. Protein concentration of the lysates was assayed using Bio-Rad protein assay kit using BSA standards.

6.5. MTT assay for cell viability

The tetrazolium reagent (MTT: 3-(4,5-dimethylthiazol-2-yl)-2,5-diphenyl-tetrazolium bromide, USB) was designed to yield a colored formazan upon metabolic reduction by viable cells [23,24]. Approximately 2×10^3 cells were plated onto each well of a 96-well plate and incubated in 5% CO_2 at 37 °C for 24 h. To assess the *in vitro* cytotoxicity, each compound was dissolved in DMSO and prepared immediately before the experiments and was diluted into the complete medium before addition to cell cultures. Test compounds were then added to the culture medium for designated various concentrations. After 48 h, an amount of 25 μL of MTT was added to each well, and the samples were incubated at 37 °C for 4 h. A 100 μL solution of lysis buffer containing 20% SDS and 50% DMF was added to each well and incubated at 37 °C for another 16 h. The absorbency at 550 nm was measured using an ELISA reader.

6.6. Secreted alkaline phosphatase (SEAP) assay

Secreted alkaline phosphatase was used as the reporting system to monitor the transcriptional activity of *hTERT* [29,30]. Here, about 2×10^3 cells each were grown in 96-well plates and incubated at 37 °C for 24 h and changed with fresh media. Varying amounts of drugs were added and cells were incubated for another 24 h. Culture media were collected and heated at 65 °C for 10 min to inactivate heat-labile phosphatases. An equal amount of SEAP buffer (2 M diethanolamine, 1 mM $MgCl_2$, and 20 mM L-homoarginine) was added to the media and *p*-nitrophenyl phosphate was added to a final concentration of 12 mM. Absorptions at 405 nm were taken, and the rate of absorption increase was determined.

6.7. Cell cultures and sulforhodamine B (SRB) assay

Human hormone-refractory prostate cancer cell line (PC-3) was from American Type Culture Collection (Rockville, MD) [25,26]. The cells were cultured in RPMI 1640 medium with 10% FBS (v/v) and penicillin (100 units/ml)/streptomycin (100 μg/ml). Cultures were maintained in a humidified incubator at 37 °C in 5% CO_2. Cells were seeded in 96-well plates in medium with 5% FBS. After 24 h, cells were fixed with 10% trichloroacetic acid to represent cell population at the time of compound addition (T_0). After additional incubation of vehicle (0.1% DMSO) or the indicated compound for 48 h, cells were fixed with 10% TCA and SRB at 0.4% (w/v) in 1% acetic acid was added to stain cells. Unbound SRB was washed out by 1% acetic acid and SRB bound cells were solubilized with 10 mM Trizma base. The absorbance was read at a wavelength of 515 nm. Using the following absorbance measurements, such as time zero (T_0), control growth (C), and cell growth in the presence of compound (T_x), the percentage growth was calculated at each of the compound concentrations levels. Percentage growth inhibition was calculated as: $100 - [(T_x - T_0)/(C - T_0)] \times 100$ for concentrations for which $T_x \geq T_0$. IC_{50} was determined at the drug concentration which resulted in 50% reduction of total protein increased in control cells during the compound incubation.

Acknowledgments

The present study was supported by National Science Council Grants NSC 100-2113-M-016, 101-2113-M-016, 100-2311-B-010-001, 98-2113-M-016-001, and National Health Research Institutes grant NHRI EX100-10050SI. We are grateful to thank NIH-NCI for their supports and to credit DTP of the NCI for performing the screening of our compounds.

Appendix A. Supplementary data

Supplementary data related to this article can be found at http://dx.doi.org/10.1016/j.ejmech.2012.11.032.

References

[1] C. Monneret, Recent developments in the field of antitumour anthracyclines, Eur. J. Med. Chem. 36 (2001) 483–493.
[2] B. Zhang, D. Qian, H.H. Ma, R. Jin, P.X. Yang, M.Y. Cai, Y.H. Liu, Y.J. Liao, H.X. Deng, S.J. Mai, H. Zhang, Y.X. Zeng, M.C. Lin, H.F. Kung, D. Xie, J.J. Huang, Anthracyclines disrupt telomere maintenance by telomerase through inducing PinX1 ubiquitination and degradation, Oncogene 31 (2012) 1–12.
[3] T.R. Cech, Beginning to understand the end of the chromosome, Cell 116 (2004) 273–279.
[4] K. Collins, Mammalian telomeres and telomerase, Curr. Opin. Cell. Biol. 12 (2000) 378–383.
[5] R.C. Allshire, M. Dempster, N.D. Hastie, Human telomeres contain at least three types of G-rich repeat distributed non-randomly, Nucleic Acids Res. 17 (1989) 4611–4627.
[6] K. Collins, J.R. Mitchell, Telomerase in the human organism, Oncogene 21 (2002) 564–579.
[7] B.S. Goueli, R. Janknecht, Regulation of telomerase reverse transcriptase gene activity by upstream stimulatory factor, Oncogene 22 (2003) 8042–8047.
[8] R. Capper, B. Britt-Compton, M. Tankimanova, J. Rowson, B. Letsolo, S. Man, M. Haughton, D.M. Baird, The nature of telomere fusion and a definition of the critical telomere length in human cells, Genes Dev. 21 (2007) 2495–2508.
[9] A. De Cian, L. Lacroix, C. Douarre, N. Temime-Smaali, C. Trentesaux, J.F. Riou, J.L. Mergny, Targeting telomeres and telomerase, Biochimie 90 (2008) 131–155.
[10] S. Neidle, Human telomeric G-quadruplex: the current status of telomeric G-quadruplexes as therapeutic targets in human cancer, FEBS J. 277 (2010) 1118–1125.
[11] S. Zimmermann, U.M. Martens, Telomeres and telomerase as targets for cancer therapy, Cell. Mol. Life Sci. 64 (2007) 906–921.
[12] R.J. O'Sullivan, J. Karlseder, Telomeres: protecting chromosomes against genome instability, Nat. Rev. Mol. Cell. Biol. 11 (2010) 171–181.
[13] H.S. Huang, T.C. Chen, R.H. Chen, K.F. Huang, F.C. Huang, J.R. Jhan, C.L. Chen, C.C. Lee, Y. Lo, J.J. Lin, Synthesis, cytotoxicity and human telomerase inhibition activities of a series of 1,2-heteroannelated anthraquinones and anthra[1,2-*d*] imidazole-6,11-dione homologues, Bioorg. Med. Chem. 17 (2009) 7418–7428.
[14] T.M. Ou, Y.J. Lu, J.H. Tan, Z.S. Huang, K.Y. Wong, L.Q. Gu, G-quadruplexes: targets in anticancer drug design, ChemMedChem 3 (2008) 690–713.
[15] S. Maiti, N.K. Chaudhury, S. Chowdhury, Hoechst 33258 binds to G-quadruplex in the promoter region of human *c-myc*, Biochem. Biophys. Res. Commun. 310 (2003) 505–512.
[16] P. Chaudhuri, B. Ganguly, S. Bhattacharya, An experimental and computational analysis on the differential role of the positional isomers of symmetric bis-2-(pyridyl)-1*H*-benzimidazoles as DNA binding agents, J. Org. Chem. 72 (2007) 1912–1923.
[17] H.S. Huang, I.B. Chen, K.F. Huang, W.C. Lu, F.Y. Shieh, Y.Y. Huang, F.C. Huang, J.J. Lin, Synthesis and human telomerase inhibition of a series of regioisomeric disubstituted amidoanthraquinones, Chem. Pharm. Bull. (Tokyo) 55 (2007) 284–292.
[18] H.S. Huang, J.F. Chiou, Y. Fong, C.C. Hou, Y.C. Lu, J.Y. Wang, J.W. Shih, Y.R. Pan, J.J. Lin, Activation of human telomerase reverse transcriptase expression by some new symmetrical bis-substituted derivatives of the anthraquinone, J. Med. Chem. 46 (2003) 3300–3307.
[19] H.S. Huang, C.L. Chou, C.L. Guo, C.L. Yuan, Y.C. Lu, F.Y. Shieh, J.J. Lin, Human telomerase inhibition and cytotoxicity of regioisomeric disubstituted amidoanthraquinones and aminoanthraquinones, Bioorg. Med. Chem. 13 (2005) 1435–1444.
[20] H.S. Huang, K.F. Huang, C.C. Lee, C.L. Chen, C.L. Li, J.J. Lin, NSC746364, NSC746365, and NSC746366: the spectra of cytotoxicity and molecular correlates of response to telomerase activity, Anti-cancer Drugs 21 (2010) 169–180.
[21] H.S. Huang, K.F. Huang, C.L. Li, Y.Y. Huang, Y.H. Chiang, F.C. Huang, J.J. Lin, Synthesis, human telomerase inhibition and anti-proliferative studies of a series of 2,7-bis-substituted amido-anthraquinone derivatives, Bioorg. Med. Chem. 16 (2008) 6976–6986.
[22] C.C. Lee, K.F. Huang, P.Y. Lin, F.C. Huang, C.L. Chen, T.C. Chen, J.H. Guh, J.J. Lin, H.S. Huang, Synthesis, antiproliferative activities and telomerase inhibition

evaluation of novel asymmetrical 1,2-disubstituted amidoanthraquinone derivatives, Eur. J. Med. Chem. 47 (2012) 323–336.
[23] T. Mosmann, Rapid colorimetric assay for cellular growth and survival: application to proliferation and cytotoxicity assays, J. Immunol. Methods 65 (1983) 55–63.
[24] F. Denizot, R. Lang, Rapid colorimetric assay for cell growth and survival. Modifications to the tetrazolium dye procedure giving improved sensitivity and reliability, J. Immunol. Methods 89 (1986) 271–277.
[25] P. Skehan, R. Storeng, D. Scudiero, A. Monks, J. McMahon, D. Vistica, J.T. Warren, H. Bokesch, S. Kenney, M.R. Boyd, New colorimetric cytotoxicity assay for anticancer-drug screening, J. Natl. Cancer Inst. 82 (1990) 1107–1112.
[26] V. Vichai, K. Kirtikara, Sulforhodamine B colorimetric assay for cytotoxicity screening, Nat. Protoc. 1 (2006) 1112–1116.
[27] D. Gomez, J.L. Mergny, J.F. Riou, Detection of telomerase inhibitors based on g-quadruplex ligands by a modified telomeric repeat amplification protocol assay, Cancer Res. 62 (2002) 3365–3368.
[28] N.W. Kim, M.A. Piatyszek, K.R. Prowse, C.B. Harley, M.D. West, P.L. Ho, G.M. Coviello, W.E. Wright, S.L. Weinrich, J.W. Shay, Specific association of human telomerase activity with immortal cells and cancer, Science 266 (1994) 2011–2015.
[29] B.R. Cullen, M.H. Malim, Secreted placental alkaline phosphatase as a eukaryotic reporter gene, Methods Enzymol. 216 (1992) 362–368.
[30] H. Seimiya, H. Sawada, Y. Muramatsu, M. Shimizu, K. Ohko, K. Yamane, T. Tsuruo, Involvement of 14-3-3 proteins in nuclear localization of telomerase, EMBO J. 19 (2000) 2652–2661.
[31] J.W. Shay, S. Bacchetti, A survey of telomerase activity in human cancer, Eur. J. Cancer 33 (1997) 787–791.
[32] J.W. Shay, W.E. Wright, Telomerase therapeutics for cancer: challenges and new directions, Nat. Rev. Drug Discov. 5 (2006) 577–584.
[33] B. Herbert, A.E. Pitts, S.I. Baker, S.E. Hamilton, W.E. Wright, J.W. Shay, D.R. Corey, Inhibition of human telomerase in immortal human cells leads to progressive telomere shortening and cell death, Proc. Natl. Acad. Sci. U. S. A 96 (1999) 14276–14281.